scientific reports

Check for updates

OPEN

The effects of systemic and sustained hypoxia on orthodontic tooth movement in rats

Kwanrat Ploysongsang[1,2,3], Yukiho Kobayashi[1]✉, Yeming Lu[1], Yuki Niki[1], Janeta Chavanavesh[2] & Keiji Moriyama[1,4]

During orthodontic tooth movement (OTM), local hypoxia on the compression side stimulates cellular remodelling of periodontal tissues. We investigated the effects of systemic, sustained hypoxia on OTM in vivo. OTM was performed on the right maxillary first molar (M1) of 8-week-old male Sprague–Dawley rats using a 10-gf nickel-titanium closed-coil spring for 4 weeks under control (21% O_2, n = 9) or hypoxic (10% O_2, n = 9) conditions. Micro-computed tomography was used to measure OTM distances, alveolar bone morphometric parameters, and M1 buccal alveolar bone levels. Osteoclast differentiation and periodontal ligament (PDL) cell proliferation were determined using tartrate-resistant acid phosphatase (TRAP) staining and immunohistochemistry, respectively. Runt-related transcription factor 2 (RUNX2) and vascular endothelial growth factor (VEGF) expression in M1 periodontal tissues were analysed using immunofluorescence. The hypoxia-OTM group showed significantly accelerated tooth movement, significantly decreased M1 buccal alveolar bone levels, significantly greater numbers of TRAP-positive cells on the compression side, and significantly reduced Ki67-positive ratios in PDL tissues. The VEGF and RUNX2 fluorescence intensities on the tension side were higher in the control-OTM than in the hypoxia-OTM group. Our results demonstrate that systemic, sustained hypoxia affects OTM by altering osteoclast and osteoblast differentiation in vivo, resulting in reduced alveolar bone levels after OTM.

Keywords Orthodontic tooth movement, Hypoxia, Periodontal ligament, Osteoblast, Osteoclast

Abbreviations

BMD	Bone mineral density
BV/TV	Bone volume fraction
H&E	Haematoxylin–eosin
HIF	Hypoxia-inducible factor
IF	Immunofluorescence
IHC	Immunohistochemistry
μCT	Micro-computed tomography
M1	Maxillary first molar
OTM	Orthodontic tooth movement
PDL	Periodontal ligament
RUNX2	Runt-related transcription factor 2
SD	Standard deviation
Tb.N	Trabecular number
Tb.Sp	Trabecular separation
Tb.Th	Trabecular thickness
TRAP	Tartrate-resistant acid phosphatase
VEGF	Vascular endothelial growth factor

[1]Department of Maxillofacial Orthognathics, Division of Maxillofacial and Neck Reconstruction, Graduate School of Medical and Dental Sciences, Institute of Science Tokyo, 1-5-45 Yushima, Bunkyo-ku, Tokyo 113-8549, Japan. [2]Department of Orthodontics, Faculty of Dentistry, Chulalongkorn University, Bangkok 10330, Thailand. [3]Institute of Science Tokyo and Chulalongkorn University International Joint Degree Doctor of Philosophy Program in Orthodontics, Tokyo, Japan. [4]Oral Science Center, Institute of Science Tokyo, Tokyo 113-8510, Japan. ✉email: yukimort@tmd.ac.jp

In orthodontic treatment, tooth movement occurs as a result of the various responses of periodontal tissues to the mechanical force applied to the dental crown, and mechanotransduction, which converts mechanical force into specific biochemical response signals of cells, plays an important role in orthodontic tooth movement (OTM). Two main theories explain the mechanism of OTM: the "pressure–tension theory" and the "distortion or bending of the alveolar bone theory"[1,2]. However, recent reports have questioned these theories[3,4]. Henneman et al. reported a theoretical model to elucidate the complex mechanisms involved in OTM[5]. In this model, the phenomena are divided into four stages: matrix strain and fluid flow, cell strain, cell activation and differentiation, and remodelling[5]. The periodontal ligament (PDL) comprises connective tissue composed of fibrous connective tissue and fluid located between the root of the tooth and the surrounding alveolar bone, and this ligament is essential for the attachment of the tooth to the alveolar bone, the dispersal of masticatory force, tooth eruption, and OTM. Recently, finite element research has attempted to model the PDL and combine biological knowledge with engineering techniques to elucidate the mechanism of OTM, but most of this research has only simulated the early stages of OTM, and only a few studies exist on long-term effects in OTM. Nowadays, not only young patients start orthodontic treatment but also patients in their 40 s and 50 s, and some of these older patients with chronic systemic diseases or smoking habits are likely to be associated with systemic hypoxia[6–8]. These reports raise questions regarding the influence of systemic hypoxia on periodontal tissue remodelling processes in OTM.

During OTM, a hypoxic environment develops on the compression side of the PDL, while aseptic inflammation and vascular obstruction occur[9], which play important roles in periodontal tissue remodelling[10,11]. Bone resorption is dominant on the compression side, whereas on the tension side, PDL tissues are stretched under tensile force, resulting in bone deposition[12]. Orthodontic forces cause the gradual compression of the PDL and lead to circulatory disturbances in PDL tissues during early stages, resulting in local hypoxia on the compression side[11,13]. We have reported that hypoxia-inducible factor (HIF)-1α expression is elevated after OTM on the compression side in rats and that PDL cells exposed to hypoxic conditions upregulate the expression of osteoclast differentiation molecules in vitro[14]. These findings suggest that the oxygen concentration may influence osteoclastogenesis in OTM[10,12,15]. Hypoxia at the compression side stimulates the production of the active transcription factor HIF-1α and activates its target genes encoding vascular endothelial growth factor (VEGF)[16–18]. HIF and its primary target VEGF play essential roles in the coupling of angiogenesis and osteogenesis during bone formation. The angiogenic factor VEGF influences osteogenic processes also via direct interactions with osteoblasts that express VEGF receptors. Osteogenic differentiation is regulated by essential transcription factors, notably runt-related transcription factor 2 (RUNX2), which governs the commitment of undifferentiated mesenchymal cells to the osteoblastic lineage. As a recognized hallmark of osteogenesis, upregulation of RUNX2 appears to play a major role in bone remodelling processes[19,20]. Hypoxic environments have been used to study the effects of hypoxia on bone metabolism[21,22]. Although different hypoxic conditions have been used, the results consistently indicate that oxygen deprivation significantly modulates osteogenic processes. Tuncay et al. reported that mild hypoxic conditions (10% O_2) increase the proliferation of osteoblasts in vitro, whereas hyperoxia (90% O_2) had the opposite effect, decreasing the proliferation rate due to the drastic change from low to high oxygen tension[11]. We have reported that periostin regulates HIF-1α levels under hypoxic conditions, resulting in the inhibition of apoptosis[23]. HIFs in gingival tissues influence the differentiation, proliferation, and apoptosis of PDL cells, osteoclasts, fibroblasts, and osteoblasts[15,24,25]. However, the precise mechanism by which hypoxia independently regulates OTM remains unclear.

To date, no study has analysed OTM in rats raised in a low-oxygen environment. Considering the relationship between hypoxia and OTM, we hypothesised that a hypoxic environment would alter the bone remodelling processes and lead to an increase in the rate of OTM via osteoclastogenesis on the compression side, together with a decrease in bone formation on the tension side. Therefore, this study aimed to evaluate the effects of systemic and sustained hypoxic conditions on OTM in vivo.

Results

Systemic hypoxia promotes OTM but inhibits alveolar bone regeneration after OTM

A 10-gf nickel-titanium closed-coil spring was applied between the right maxillary first molar (M1) and the maxillary incisors to induce mesial tooth movement of the M1 for 28 days (Fig. 1A, B). The left M1 served as the non-OTM side. In the hypoxia group, the animals were kept in a controlled-atmosphere hypoxic animal chamber with an oxygen level of 10% (Fig. 1C). Comparing the control-OTM and hypoxia-OTM groups, the hypoxia-OTM group showed a significantly higher distance of OTM (Fig. 2A, C). Both control-OTM and hypoxia-OTM groups showed lower trabecular separation (Tb.Sp) than their corresponding non-OTM groups; the non-OTM side also showed a difference between the control and hypoxia groups, as the hypoxia-non-OTM group had a significantly higher Tb.Sp than the control-non-OTM group (Fig. 2D). Trabecular thickness (Tb.Th) was increased in the OTM group compared to that in the non-OTM group, but no significant difference was observed between the control-OTM and hypoxia-OTM groups (Fig. 2D). In addition, the hypoxia-non-OTM and hypoxia-OTM groups significantly differed in their bone volume fractions (BV/TVs), with no significant difference between the control-OTM and hypoxia-OTM groups (Fig. 2D). Bone mineral density (BMD) and trabecular number (Tb.N) showed no significant differences between the groups, although hypoxia resulted in lower Tb.N in both non-OTM and OTM groups (Fig. 2D). The alveolar bone level on the buccal surface in the hypoxia-OTM group, determined as the distance from the cementoenamel junction to the alveolar crest after OTM, was significantly greater than that in the other groups, and a decrease in the alveolar bone level was observed (Fig. 3A, B).

OTM under hypoxic conditions promotes osteoclastogenesis on the compression side

Histological examination using haematoxylin–eosin (H&E) staining revealed that the PDLs on the tension side of the control-OTM group exhibited a more systematically arranged cellular architecture than those of the

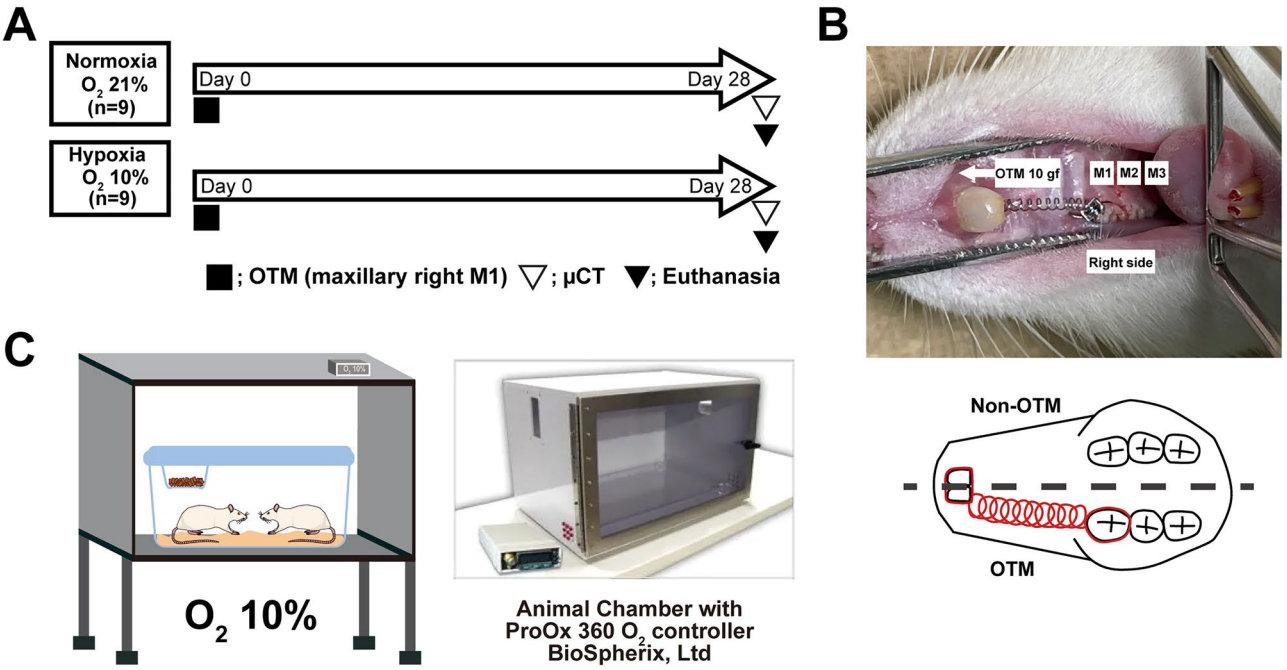

Fig. 1. Representative illustration of the experimental course, an intraoral image of orthodontic tooth movement (OTM) in rats, and the animal chamber used for the in vivo hypoxia experiment. (**A**) Experimental time course of the 4-week study period. (**B**) OTM in rats is performed on the right maxillary first molar (M1) with a NiTi closed-coil spring of 10 gf to mesialise the M1. (**C**) Representative image of the hypoxic animal chamber using 10% oxygen concentration to simulate systemic and sustained hypoxia.

hypoxia-OTM group (Fig. 4A). Histological evaluation using toluidine blue staining demonstrated osteoblastic cell alignment along the osteogenic front of the alveolar bone of the tension side in OTM groups. The osteoblastic cell arrangement was more pronounced in the control-OTM group than in the hypoxia-OTM group (Fig. 4B). Tartrate-resistant acid phosphatase (TRAP) staining revealed osteoclastic activity within the PDL of the compression side (Fig. 4C). In the non-OTM group, TRAP-positive cells were predominantly localised to the distal side caused by the physiological distal drift of rat molars, with a significant difference between the control-non-OTM and hypoxia-non-OTM groups (Fig. 4C). Similarly, on the compression side of the OTM group, a significant difference of the number of TRAP-positive cells was observed between the control-OTM and hypoxia-OTM groups (Fig. 4C). Analyses of the number of TRAP-positive cells on the mesial and tension sides revealed no significant differences between the control-OTM and hypoxia-OTM groups (Fig. 4C). Notably, both the hypoxia-non-OTM and hypoxia-OTM groups showed significantly higher numbers of TRAP-positive cells than their respective controls (Fig. 4D).

OTM under hypoxic conditions suppresses PDL cell proliferation as well as RUNX2 and VEGF expression

Quantitative analyses revealed significant differences in the distribution of Ki67-positive cells between the tension and compression areas in both control-OTM and hypoxia-OTM groups, with significantly increased numbers of Ki67-positive cells on the tension side (Fig. 5A, B). In addition, the control groups had consistently higher numbers of Ki67-positive cells than their hypoxic counterparts in both non-OTM and OTM groups (Fig. 5A). Statistical analyses revealed significant differences in RUNX2 fluorescence intensity between the tension side of the control-OTM and hypoxia-OTM groups, which paralleled the differences in the mesial regions of the control-non-OTM and hypoxia-non-OTM groups (Fig. 6A). Quantitative assessments showed that the control group exhibited increased fluorescence intensity on both mesial and tension sides (Fig. 6B). Consistent with this observation, immunofluorescence (IF) analysis of VEGF expression revealed a significantly higher intensity on the tension side of the control-OTM group than on that of the hypoxia-OTM group (Fig. 6C, D).

Discussion

To investigate the effects of sustained hypoxia on OTM, we established a rat model using a 10-gf closed-coil spring on the right M1 for 4 weeks. This mild force was selected to induce detectable tooth movement while minimising root resorption and facilitating bone formation on the tension side[26–28]. In this study, the OTM distance was significantly greater in the hypoxia-OTM group than in the control-OTM group. Moreover, the buccal alveolar bone level of the M1 was significantly lower in the hypoxia-OTM group than in any other group. These data suggest that hypoxia may upregulate bone resorption and osteoclast differentiation during the bone remodelling process of OTM. The number of TRAP-positive cells was significantly higher on the compression side in the hypoxia group than in the control group. These results are consistent with those of a previous study by

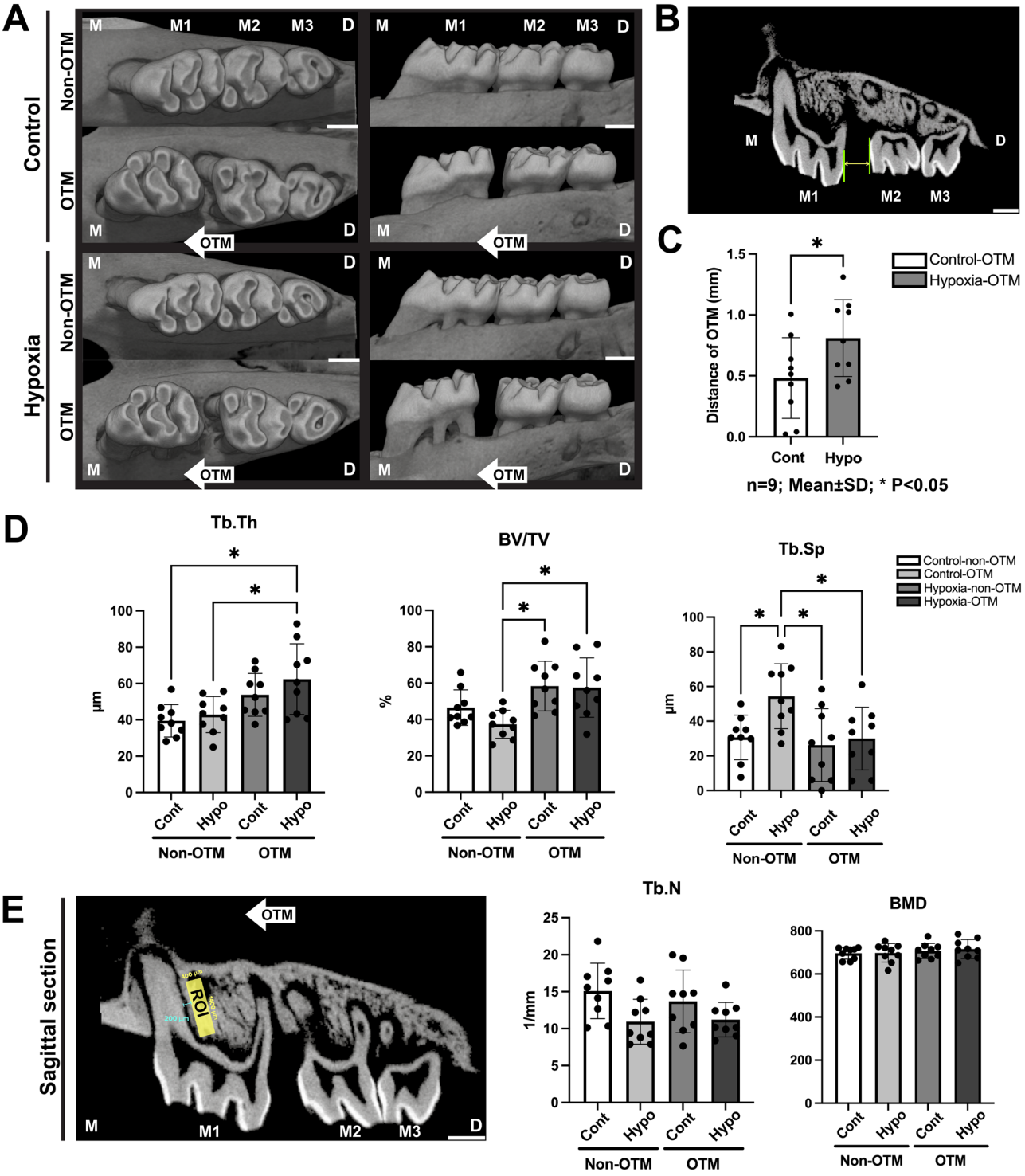

Li et al., who investigated whether compression and hypoxia influence osteoclastogenesis within PDL cells and concluded that both compressive force and hypoxia are involved in the initiation of osteoclastogenesis in OTM and may have combinatorial effects[15].

Combined hypoxia-OTM effects on bone formation

To evaluate bone formation, we also analysed several bone morphometric parameters using 3D X-ray microtomography (μCT) of the distal area of the M1 mesial root and compared these parameters between experimental groups. The OTM group showed reduced Tb.Sp owing to bone formation on the tension side, whereas the hypoxia-non-OTM group showed, owing to physiological distal compression, a significantly higher Tb.Sp. Tb.Th increased in the OTM group compared to the non-OTM group, but the control-OTM and hypoxia-OTM groups did not significantly differ. Despite the significant difference in BV/TV between the hypoxia-non-OTM and hypoxia-OTM groups, no significant difference was observed between the control-OTM and hypoxia-OTM groups. The BMD did not differ significantly between the groups, suggesting that hypoxia did not

◂**Fig. 2**. Representative examples of three-dimensional (3D) micro-CT (μCT) images and the distance of OTM to display the mesial movement of the M1. Comparing the four study groups (control-non-OTM, control-OTM, hypoxia-non-OTM, and hypoxia-OTM), a significantly higher distance of tooth movement can be observed in the hypoxia-OTM group. The morphometric parameters of the trabecular bone for quantitative analyses and the area of interest are shown in the sagittal section. No significant difference is observed between control-OTM and hypoxia-OTM. (**A**) Occlusal and buccal views of OTM compared between control and hypoxia groups on both non-OTM and OTM sides. Scale bar, 1 mm. (**B**) Representative image of an OTM measurement. The distance between the most distal point of the upper right M1 crown and the most mesial point of the M2 crown is shown. Scale bar, 1 mm. (**C**) Comparison of the OTM distance between the control-OTM and hypoxia-OTM groups. n = 9; mean ± standard deviation (SD); * $p < 0.05$. (**D**) Analysis of the 3D microarchitecture using μCT scans of the trabecular bone. Trabecular thickness (Tb.Th), bone volume fraction (BV/TV), trabecular separation (Tb.Sp), trabecular number (Tb.N), and bone mineral density (BMD) are compared among the four study groups control-non-OTM, control-OTM, hypoxia-non-OTM, and hypoxia-OTM. n = 9; mean ± SD; * $p < 0.05$. (**E**) Representative image of the region of interest (ROI) for analysis. The rectangular volume size of 400 μm × 400 μm × 1400 μm is located in the distal area of the alveolar bone adjacent to the mesial root of M1. The evaluated area is 200 μm from the root surface. Scale bar, 1 mm.

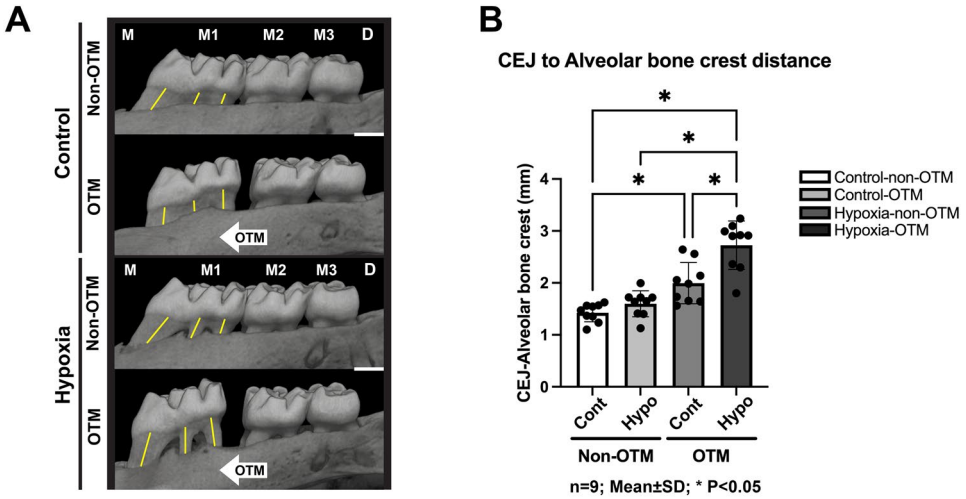

Fig. 3. μCT images of the buccal alveolar bone level of M1 at the end of the experiment. The hypoxia-OTM group shows a significantly greater distance from the cementoenamel junction (CEJ) to the alveolar crest, and a decrease in the alveolar bone level is observed. (**A**) Representative μCT images of the buccal alveolar bone level after OTM compared to the control side. The yellow lines represent the total distance from the CEJ to the alveolar crest, measured at three sites. (**B**) Measurement of the alveolar bone level and comparison among the four experimental groups. Scale bar, 1 mm. n = 9; mean ± SD; * $p < 0.05$.

affect bone quality itself. The hypoxia group showed a lower Tb.N, although no significant difference in Tb.N was observed between groups. Bone formation may be caused by an increase in Tb.Th rather than Tb.N. In a previous study[28], the μCT results after OTM intervention in the normal oxygen environment were consistent with our finding that Tb.Th and BV/TV were greater in the OTM group than in the non-OTM group. The effects of hypoxia on bone strength in rats have been reported previously. BMD, BV/TV, Tb.Th, and Tb.N were lower in the hypobaric hypoxia group than in the normoxia group[22]. Given the lack of comprehensive studies analysing bone morphometric parameters after combined hypoxic exposure and OTM, our results suggest that, although sustained hypoxia may affect bone morphology, the characteristic bone remodelling response and tensile osteogenesis associated with OTM may counterbalance any substantial changes in bone architectural parameters.

Cell activity changes involved in bone remodelling

Histological observations with H&E showed tensile force-induced cell stretching on the tension side in both control-OTM and hypoxia-OTM groups. Notably, the PDL on the tension side of the control-OTM group showed a systematically arranged cellular architecture compared with that of the hypoxia-OTM group. This indicates that hypoxic intervention may cause cell irregularities and disorders. TRAP staining was performed to quantify multinucleated osteoclast differentiation. On the distal side of non-OTM specimens, TRAP-positive cells showed predominant localisation due to the physiological distal drift characteristic of rat molars[29]. A significant difference was observed between the control-OTM and hypoxia-non-OTM groups. Similarly, a significant difference was observed between the control and hypoxic groups on the compression side of the OTM

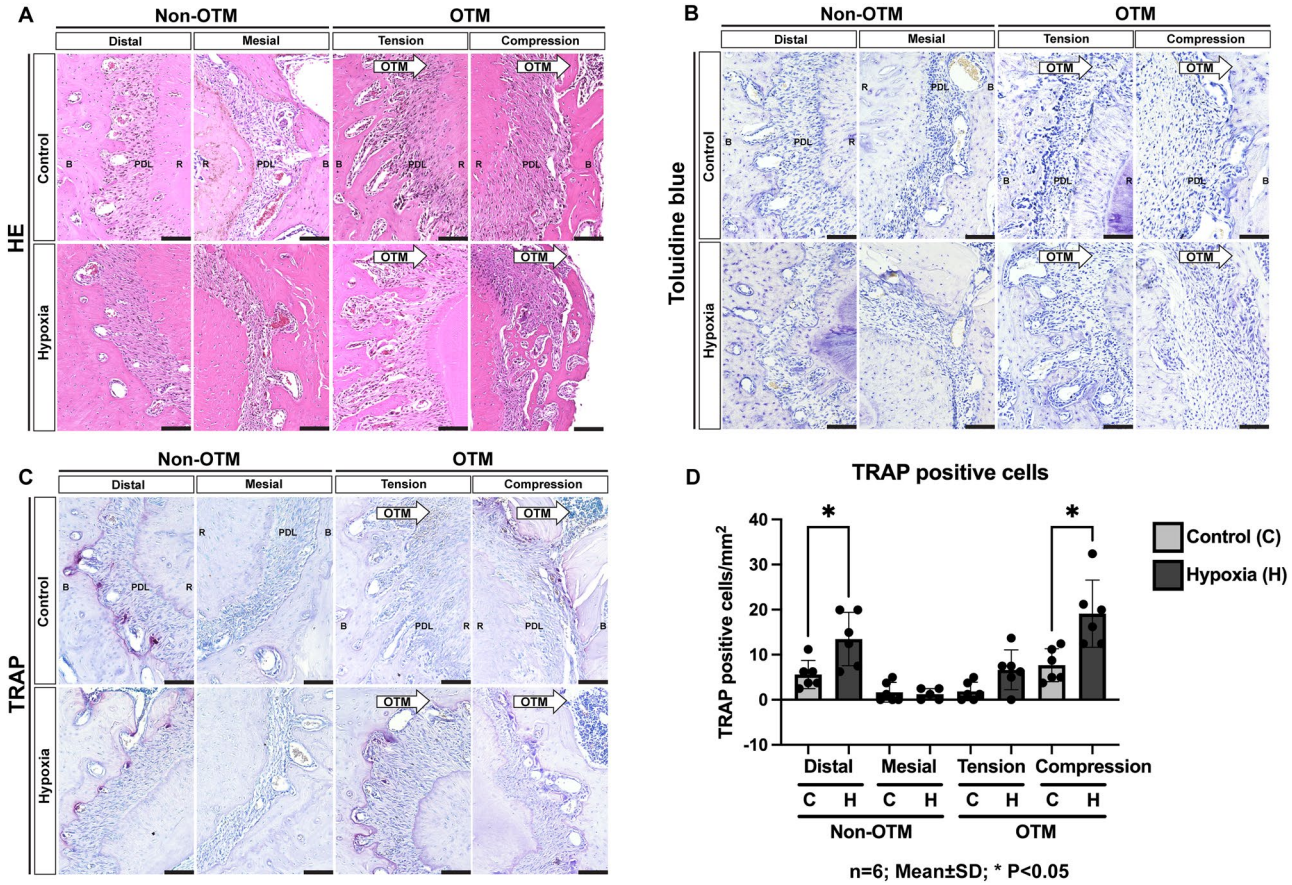

Fig. 4. Histological images of the haematoxylin–eosin (H&E), toluidine blue, and tartrate-resistant acid phosphatase (TRAP) stainings of the mesial root of M1, the distal and mesial sides in the non-OTM group or the tension and compression sides of the OTM group, with the quantitative analysis of the area positive for TRAP staining. (**A**) Representative H&E-stained images. The periodontal ligament (PDL) is stretched on the tension side of the OTM section and shows a more systematically arranged cellular architecture compared to its hypoxia-OTM counterpart. (**B**) Representative toluidine blue-stained images. The osteoblastic cell lining is pronounced on the tension side of the control-OTM specimen. (**C**) Representative TRAP-stained images showing the expression of multinucleated osteoclast activity, particularly on the compression side of the OTM specimen and the distal side of the non-OTM specimen. (**D**) Quantitative analysis of TRAP-positive cells comparing the control (C) and hypoxia (H) groups. The graph represents the number of TRAP-positive cells specifically on the distal-mesial side of the non-OTM group along with the tension–compression side of the OTM group. Scale bar, 100 μm. n = 6; mean ± SD; * $p < 0.05$.

group. These findings suggest that hypoxic conditions modulate osteoclastic differentiation and accelerate bone-resorptive processes. This hypothesis was supported by concurrent analyses of the buccal alveolar bone levels.

In addition, the basic thiazine metachromatic dye toluidine blue was used to detect osteoblasts in paraffin sections[30]. Sections on the tension side of the control-OTM group showed prominent osteoblastic lining which differed markedly from those of the hypoxia-OTM group. This finding implies that hypoxic conditions affect osteoblastic differentiation, particularly on the tension side. To elucidate the influence of hypoxic conditions on bone formation, we performed immunohistochemical (IHC) analyses of Ki67 to assess cellular proliferation dynamics. Our results showed a significant reduction in Ki67-positive cell populations among osteoblasts and PDL cells in the hypoxia group compared to those in the control group after OTM. Under non-OTM conditions, the physiological distal drift of the rat molars induced mild mesial stretching, resulting in a slightly higher number of Ki67-positive cells in the control group, although this difference was not significant. These cellular observations suggest that sustained hypoxic exposure may suppress cellular proliferative mechanisms during bone remodelling and periodontal tissue remodelling.

Angiogenesis and osteogenesis

IF stainings of RUNX2 and VEGF were performed to examine osteoblastic differentiation and angiogenesis. RUNX2 is a multifunctional transcription factor that controls skeletal development by regulating chondrocyte and osteoblast differentiation. During osteoblast differentiation, RUNX2 regulates the gene expression of bone matrix proteins. IF analysis revealed significant changes in RUNX2 expression, with significantly reduced intensity on the tension side of hypoxia-OTM sections compared to that of control-OTM sections. A similar

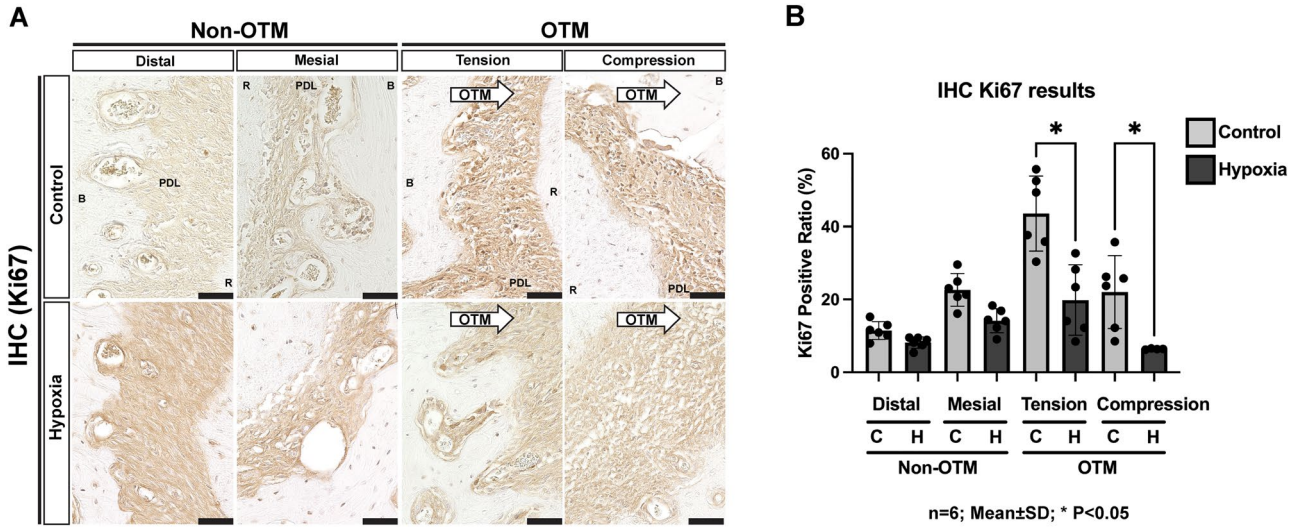

Fig. 5. Immunohistochemistry (IHC) sections of Ki67 staining of the mesial root of M1, including the distal and mesial side of the non-OTM group and the tension and compression sides of the OTM group. The quantitative results of the Ki67-positive ratio (%) show significant differences between tension and compression areas in both control-OTM and hypoxia-OTM groups. The control groups have consistently higher numbers of Ki67-positive cells compared to their hypoxic counterparts in the non-OTM and OTM groups. (**A**) Representative image of IHC staining for Ki67. (**B**) Quantitative comparison of Ki67-positive cells (%) between groups. The Ki67-positive ratio in the hypoxia-OTM group is significantly lower on both the tension and compression sides compared with that in the control-OTM group. Scale bar, 100 μm. n = 6; mean ± SD; * $p < 0.05$.

pattern of decreased RUNX2 expression was observed on the mesial side in the non-OTM group. These results suggest that sustained hypoxic conditions suppress osteoblastic differentiation, as manifested by the decreased IF intensity of RUNX2. Our results are consistent with previous findings[31] documenting RUNX2 induction after tooth movement on the mesial side of the control groups, highlighting the potential modulatory effect of hypoxia on the expression of critical osteogenic transcription factors. VEGF and its relationship with osteogenesis in OTM have been the subject of many previous publications[32–34]. According to Militi et al., the VEGF staining pattern decreases between 7 and 14 days on both the compression and tension sides but increases between 14 and 30 days on both the compression and tension sides[33]. This suggests that regenerative processes occur during this period, as new bone and vascular structures are formed. HIFs are activated in low-oxygen environments and increase VEGF levels in mature osteoblasts. VEGF then promotes angiogenesis by acting on endothelial cells and increasing the supply of oxygen and nutrients needed for bone formation. The HIF–VEGF pathway is critical for linking new blood vessel formation to bone growth[35]. In our results, the tension sides of the hypoxia-OTM group showed a significant reduction in VEGF intensity. This may indicate that hypoxic conditions, together with OTM, can reduce the amount of angiogenesis and lead to less osteogenesis on the OTM tension side.

Limitations

The rat model under hypoxic conditions may differ from humans regarding oxygen tolerance thresholds and cellular adaptation mechanisms. Biomechanical forces applied experimentally may not accurately reflect those in human orthodontics due to anatomical and physiological differences between these two species. The characteristics of bone remodelling processes also vary between rats and humans, constraining direct clinical application of our findings. Future investigations should develop experimental approaches that better approximate human orthodontic conditions to address these translational gaps. Nevertheless, our research provides essential foundational knowledge about underlying biological mechanisms that can guide subsequent clinical studies in orthodontics.

Conclusions

To our knowledge, this is the first study investigating the effects of systemic and sustained hypoxia on OTM in rats. Our results indicate that systemic hypoxia influences osteoclast differentiation in vivo, enhancing osteoclast activity, particularly on the compression side of the OTM, while inhibiting osteoblast and PDL cell proliferation, resulting in decreased alveolar bone height after OTM. Significant differences were observed in the IHC of Ki67 and the IF of RUNX2 and VEGF. These results suggest that hypoxia plays a critical role in the remodelling of PDL tissues during OTM.

Methods

All experiments were carried out in accordance with relevant guidelines and regulations. All animal experiments were reviewed and approved by the Institutional Animal Care and Use Committee of the Institute of Science,

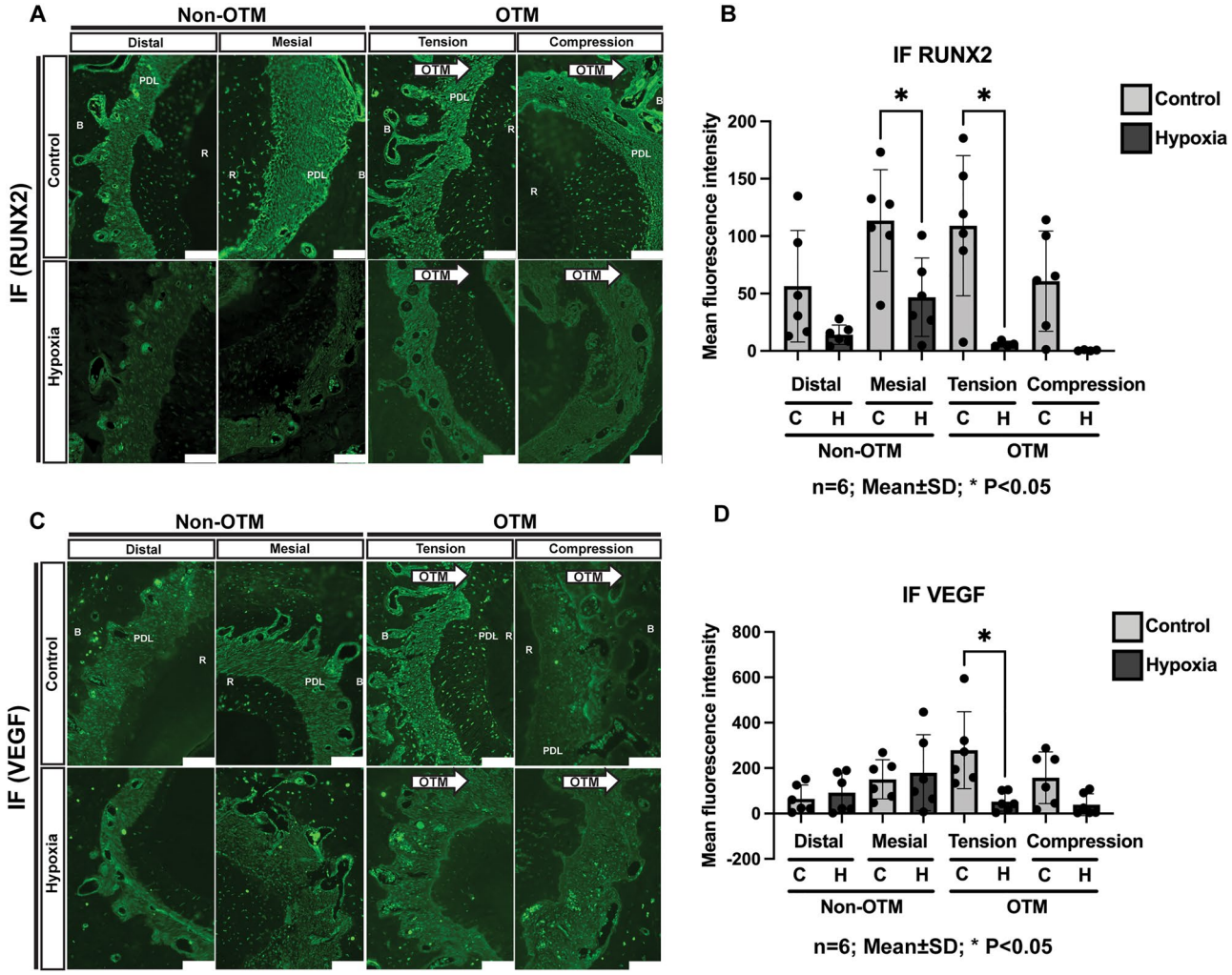

Fig. 6. Immunofluorescence (IF) staining and quantitative analysis of runt-related transcription factor 2 (RUNX2) expression comparing the tensile regions of the control-OTM and hypoxia-OTM groups and between the mesial regions of the control-non-OTM and hypoxia-non-OTM groups. Moreover, the fluorescence intensity indicating vascular endothelial growth factor (VEGF) expression is compared between the tensile regions of the control-OTM and hypoxia-OTM groups. (**A**) Representative IF image stained for RUNX2. (**B**) Quantitative analysis of RUNX2 mean fluorescence intensity compared between each group. n = 6; mean ± SD; * $p < 0.05$. (**C**) Representative IF image stained for VEGF. (**D**) Quantitative analysis of VEGF fluorescence intensity compared between each group. Scale bar, 100 μm. n = 6; mean ± SD; * $p < 0.05$.

Tokyo, Japan (approval no. A2023-155A) and followed institutional policy guidelines. This study adhered to the ARRIVE (Animal Research: Reporting of In Vivo Experiments) guidelines.

Animals

The sample size was calculated using the mean and standard deviation (SD) of a previous study that investigated alveolar bone changes during OTM[28]. According to the calculations performed using the G* Power software version 3.1, at least four rats per group were required. The number of rats analysed in our experiments determined the sample size for the in vivo study. Therefore, each group comprised nine rats. Eight-week-old male Sprague–Dawley rats shipped at seven weeks of age were used in this study (Oriental Yeast Co., Ltd., Tokyo, Japan). Rats were maintained under a 12-h light/dark cycle at 22–24 °C and 50 ± 5% humidity with ad libitum water and soft food and were acclimated to the environment for 1 week prior to the start of the experiment. The rats were randomly divided into control and hypoxia groups. Rats were euthanized with 100% CO_2 inhalation at a fill rate of 30–70% displacement of chamber volume per minute with CO_2.

OTM of the right maxillary first molar in rat

All animals were anaesthetised with a subcutaneous injection of a general anaesthetics mix consisting of 0.15 mg/kg medetomidine 2% (Domitor®, Nippon Zenyaku Kogyo Co., Ltd., Tokyo, Japan), 2.0 mg/kg midazolam 8% (Sandoz®, Fuji Pharma Co, Ltd. Tokyo, Japan), and 2.5 mg/kg butorphanol 10% (Vetorphale®, Meiji Animal Health Co, Ltd, Tokyo, Japan) before placing a 10-gf nickel-titanium closed-coil spring (Tomy International,

Tokyo, Japan) between the right M1 and the maxillary incisors to induce mesial tooth movement of the M1 for 28 days (Fig. 1A). A groove was created in the cervical area of the central incisors, tied with a ligature wire, and fixed with a light-cured resin composite (Transbond, Unitek/3 M). The left M1 served as the non-OTM side (Fig. 1B). Reactivation was not performed during the experimental period after the placement of the closed-coil spring. Soft food was fed from the day of the OTM experiment to reduce the risk of injury and damage to the orthodontic appliance. The appliance was also checked daily, and the central incisors were cut to prevent appliance breakage. If the ligature wire was loosened, a new ligature wire was placed using the former closed-coil spring. The body weights of the rats were measured on the first day of the experiment, every 4 days, and on the day of euthanasia (Supplementary Fig. S1).

Hypoxic environments during OTM

In the control group, the animals were maintained in a normoxic environment with an oxygen level of 21%. In the hypoxia group, the animals were kept in a controlled-atmosphere hypoxic animal chamber with an oxygen level of 10% (animal chamber with ProOx 360 O_2 controller; BioSpherix, Ltd.; Fig. 1C).

Histological sample preparation and histological analysis

The samples were divided into four groups (n = 9 each): control-non-OTM, control-OTM, hypoxia-OTM, and hypoxia-non-OTM. Histological changes were evaluated using H&E staining, toluidine blue staining, TRAP staining, IHC staining for Ki67, and IF staining for VEGF and RUNX2 (n = 6). After euthanasia, the maxillae were immediately dissected and fixed at 4 °C in 4% paraformaldehyde for 7 days which was subsequently replaced with 70% ethanol. The dissected rat maxillae were decalcified with 18% EDTA (pH 7.4) (G-Chelate Mild; GenoStaff, Tokyo, Japan) at 4 °C for 10 weeks, dehydrated using graded alcohol, and embedded in paraffin. Serial 7-µm thick transverse sections were prepared. Sections were mounted on coated glass slides, deparaffinized with G-NOX (alternative xylene; GenoStaff), and stained with H&E. Toluidine blue staining was also used to observe the osteoblasts in the osteogenic front on the tension side of the PDL. To analyse multinucleated osteoclast activity on the alveolar bone, sections were deparaffinized, rehydrated, and stained using a TRAP/alkaline phosphatase staining kit (No. 294-67001; Wako, Japan), according to the manufacturer's instructions. The number of TRAP-positive multinucleated osteoclasts in the PDL area around the mesial root of M1 was counted by a single examiner using three randomised sections of each sample, and the averages were calculated for analysis. Sections from each group were stained with Ki67 primary antibody (1:200, ab15580; Abcam, Cambridge, UK) for IHC analysis. After deparaffinization and rehydration, the sections were processed with antigen retrieval for 40 min at 75 °C (HistoVT One, Nacalai Tesque, Kyoto, Japan) and treated with 0.3% hydrogen peroxide in methanol for 30 min, followed by skim milk as a blocking buffer for 1 h. The sections were then incubated with primary antibody for 2 h at room temperature. The secondary antibody was applied with a biotinylated pan-specific universal antibody (VECTASTAIN® Universal Quick HRP kit, PK-7800, Vector Labs, CA, USA) for 10 min. Sections were then stained with 3,3′-diaminobenzidine (DAB) substrate (ImmPACT DAB Peroxidase, SK-4105, Vector Labs) and counterstained with haematoxylin. The Ki67-positive ratio (%) was determined using ImageJ software (National Institutes of Health, Bethesda, Maryland, USA). The four groups were quantitatively compared by a single investigator using three randomly selected areas of the sections of each sample, and the averages were calculated for analysis. The expression of RUNX2 and VEGF was evaluated by IF staining with RUNX2 polyclonal antibody (1:200, PA587299, Invitrogen) and VEGF antibody (1:100, 19003-1-AP, Proteintech). Deparaffinized and rehydrated sections were processed with Proteinase K (20 mg/ml, ab64220, Abcam, Cambridge, UK) for antigen retrieval for 5–7 min at room temperature and permeabilised with 0.1–0.2% Triton in phosphate-buffered saline and a blocking agent with G-Block (GB-01, GenoStaff). Sections were incubated with primary antibodies against RUNX2 and VEGF overnight at 4 °C. The sections were incubated with secondary antibodies (goat anti-rabbit IgG H&L Alexa Fluor® 594; ab150080; Abcam) for 60 min at room temperature. Sections were mounted for fluorescence labelling with DAPI (VECTASHIELD® PLUS Antipode Mounting Medium with DAPI; H-2000, Vector Labs) according to the kit instructions. Morphological and histological changes and IF intensities were observed using light microscopy and imaging software (BZ-X800; Keyence Corporation, Osaka, Japan). All sections were categorized into one of the four study groups; for more detailed analyses, non-OTM sections were divided into distal and mesial sides, whereas OTM sections were divided into tension and compression sides.

µCT analysis

The maxillae were scanned through a 0.1-mm filtered brass plate using a microfocus X-ray CT system (SMX-100CT; Shimadzu, Kyoto, Japan) at 70 kV, 114 µA, and 0.022 mm/voxel based on previous reports[28,31,36,37]. Three-dimensional µCT images were reconstructed using image analysis software (TRI/3D-BON; Ratoc System Engineering Co., Ltd., Osaka, Japan). The OTM distance was measured as the distance between the most distal surface of the crown of the right M1 and the most mesial surface of the crown of the right maxillary second molar (M2) using 2D imaging and ImageJ software (Fig. 2B). The distance was measured three times to determine the average amount of tooth movement in each experimental group. For alveolar bone analysis, rectangular volumes of 400 µm width × 400 µm thickness × 1400 µm height of the alveolar bone adjacent to the mesial roots of M1 were selected as regions of interest to assess the trabecular bone in the bone formation area of the tension side (Fig. 2E). The evaluated area was 200 µm from the root surface to exclude the PDL space. The positions of the rectangular volumes and regions of interest were adapted from previous reports[38–41]. As 3D microarchitectural parameters of the trabecular bone, BV/TV, Tb.Th, Tb.N, Tb.Sp, and BMD were measured using the 3D µCT image. Moreover, changes in the buccal alveolar bone level, represented at the alveolar bone crest on the buccal surface of M1, were measured as the total three-site distance from the cementoenamel junction to the alveolar

bone crest on both non-OTM and OTM sides, comparing the control and hypoxia groups according to a previous study[42].

Statistical analysis

All data are expressed as the mean and SD. Statistical analyses were performed using GraphPad Prism version 10.2 (GraphPad Software Inc., La Jolla, CA, USA). The Shapiro–Wilk test was used to assess the normal distribution of the data. A paired t-test was performed to compare the OTM distances between control-OTM and hypoxia-OTM groups. One-way analysis of variance (ANOVA) followed by Bonferroni's multiple comparison test was used to compare bone morphometric parameters and buccal alveolar bone levels among the control-non-OTM, control-OTM, hypoxia-non-OTM, and hypoxia-OTM groups. ANOVA followed by Bonferroni's multiple comparison test was also used to compare the number of TRAP-positive cells, number of Ki67-positive cells, and IF intensity of RUNX2 between the control and hypoxia groups, specifically on the mesial-distal side of non-OTM groups and the tension–compression side of OTM groups. The Kruskal–Wallis test followed by Dunn's multiple comparison test was used to compare the IF intensity of VEGF. Statistical significance was set at $p < 0.05$.

Data availability

The data that support the findings of this study are available from the corresponding author, Y.K., upon reasonable request.

Received: 11 March 2025; Accepted: 18 June 2025
Published online: 01 July 2025

References

1. Reitan, K. The initial tissue reaction incident to orthodontic tooth movement as related to the influence of function; an experimental histologic study on animal and human material. *Acta Odontol. Scand. Suppl.* **6**, 1–240 (1951).
2. Schwarz, A. M. Tissue changes incidental to orthodontic tooth movement. *Int. J. Orthodont. Oral Surg. Radiogr.* **18**, 331–352 (1932).
3. Cattaneo, P. M., Dalstra, M. & Melsen, B. The finite element method: a tool to study orthodontic tooth movement. *J. Dent. Res.* **84**, 428–433 (2005).
4. Melsen, B. Biological reaction of alveolar bone to orthodontic tooth movement. *Angle Orthod.* **69**, 151–158 (1999).
5. Henneman, S., Von den Hoff, J. W. & Maltha, J. C. Mechanobiology of tooth movement. *Eur. J. Orthod.* **30**, 299–306 (2008).
6. Barnes, L., Mesarwi, O. & Sanchez-Azofra, A. The cardiovascular and metabolic effects of chronic hypoxia in animal models: A mini-review. *Front. Physiol.* **13**, 873522 (2022).
7. Lee, H. et al. Cigarette smoke-mediated oxidative stress induces apoptosis via the MAPKs/STAT1 pathway in mouse lung fibroblasts. *Toxicol. Lett.* **240**, 140–148 (2016).
8. Sancilio, S., Gallorini, M., Cataldi, A. & di Giacomo, V. Cytotoxicity and apoptosis induction by e-cigarette fluids in human gingival fibroblasts. *Clin. Oral Investig.* **20**, 477–483 (2016).
9. Niklas, A., Proff, P., Gosau, M. & Romer, P. The role of hypoxia in orthodontic tooth movement. *Int. J. Dent.* **2013**, 841840 (2013).
10. Park, H. J. et al. Hypoxia inducible factor-1alpha directly induces the expression of receptor activator of nuclear factor-kappaB ligand in periodontal ligament fibroblasts. *Mol. Cells* **31**, 573–578 (2011).
11. Tuncay, O. C., Ho, D. & Barker, M. K. Oxygen tension regulates osteoblast function. *Am. J. Orthod. Dentofac. Orthop.* **105**, 457–463 (1994).
12. Chae, H. S. et al. The effect of antioxidants on the production of pro-inflammatory cytokines and orthodontic tooth movement. *Mol. Cells* **32**, 189–196 (2011).
13. Kitase, Y. et al. Analysis of gene expression profiles in human periodontal ligament cells under hypoxia: the protective effect of CC chemokine ligand 2 to oxygen shortage. *Arch. Oral Biol.* **54**, 618–624 (2009).
14. Jindarojanakul, P. et al. Changes in superoxide dismutase 3 (SOD3) expression in periodontal tissue during orthodontic tooth movement of rat molars and the effect of SOD3 on in vitro hypoxia-exposed rat periodontal ligament cells. *Eur. J. Orthod.* **45**, 430–437 (2023).
15. Li, M. L. et al. Compression and hypoxia play independent roles while having combinative effects in the osteoclastogenesis induced by periodontal ligament cells. *Angle Orthod.* **86**, 66–73 (2016).
16. Arnett, T. R. et al. Hypoxia is a major stimulator of osteoclast formation and bone resorption. *J. Cell Physiol.* **196**, 2–8 (2003).
17. Huang, H., Williams, R. C. & Kyrkanides, S. Accelerated orthodontic tooth movement: molecular mechanisms. *Am. J. Orthod. Dentofac. Orthop.* **146**, 620–632 (2014).
18. Romer, P., Wolf, M., Fanghanel, J., Reicheneder, C. & Proff, P. Cellular response to orthodontically-induced short-term hypoxia in dental pulp cells. *Cell Tissue Res.* **355**, 173–180 (2014).
19. Oishi, S. et al. Intermittent hypoxia influences alveolar bone proper microstructure via hypoxia-inducible factor and VEGF expression in periodontal ligaments of growing rats. *Front. Physiol.* **7**, 416 (2016).
20. Schipani, E., Maes, C., Carmeliet, G. & Semenza, G. L. Regulation of osteogenesis-angiogenesis coupling by HIFs and VEGF. *J. Bone Miner. Res.* **24**, 1347–1353 (2009).
21. Hao, X. et al. Bone deterioration in response to chronic high-altitude hypoxia is attenuated by a pulsed electromagnetic field via the primary cilium/HIF-1alpha axis. *J. Bone Miner. Res.* **38**, 597–614 (2023).
22. Wang, W. et al. The hypobaric hypoxia environment impairs bone strength and quality in rats. *Int. J. Clin. Exp. Med.* **10**, 9397–9406 (2017).
23. Aukkarasongsup, P., Haruyama, N., Matsumoto, T., Shiga, M. & Moriyama, K. Periostin inhibits hypoxia-induced apoptosis in human periodontal ligament cells via TGF-β signaling. *Biochem. Biophys. Res. Commun.* **441**, 126–132 (2013).
24. Wu, Y. et al. The osteogenic differentiation of PDLSCs is mediated through MEK/ERK and p38 MAPK signalling under hypoxia. *Arch. Oral Biol.* **58**, 1357–1368 (2013).
25. Xiao, Z., Han, Y., Zhang, Y. & Zhang, X. Hypoxia-regulated human periodontal ligament cells via Wnt/beta-catenin signaling pathway. *Medicine* **96**, e6562 (2017).
26. Gonzales, C. et al. An in vivo 3D micro-CT evaluation of tooth movement after the application of different force magnitudes in rat molar. *Angle Orthod.* **79**, 703–714 (2009).
27. Gonzales, C. et al. Force magnitude and duration effects on amount of tooth movement and root resorption in the rat molar. *Angle Orthod.* **78**, 502–509 (2008).
28. Ru, N., Liu, S. S., Zhuang, L., Li, S. & Bai, Y. In vivo microcomputed tomography evaluation of rat alveolar bone and root resorption during orthodontic tooth movement. *Angle Orthod.* **83**, 402–409 (2013).

29. Tsuchiya, S. et al. Physiological distal drift in rat molars contributes to acellular cementum formation. *Anat. Rec.* **296**, 1255–1263 (2013).
30. Sridharan, G. & Shankar, A. A. Toluidine blue: A review of its chemistry and clinical utility. *J. Oral Maxillofac. Pathol.* **16**, 251–255 (2012).
31. Pan, J. et al. Lithium enhances alveolar bone formation during orthodontic retention in rats. *Orthod. Craniofac. Res.* **20**, 146–151 (2017).
32. Di Domenico, M. et al. Cytokines and VEGF induction in orthodontic movement in animal models. *J. Biomed. Biotechnol.* **2012**, 201689 (2012).
33. Militi, A. et al. An immunofluorescence study on VEGF and extracellular matrix proteins in human periodontal ligament during tooth movement. *Heliyon* **5**, e02572 (2019).
34. Miyagawa, A., Chiba, M., Hayashi, H. & Igarashi, K. Compressive force induces VEGF production in periodontal tissues. *J. Dent. Res.* **88**, 752–756 (2009).
35. Fan, L., Li, J., Yu, Z., Dang, X. & Wang, K. The hypoxia-inducible factor pathway, prolyl hydroxylase domain protein inhibitors, and their roles in bone repair and regeneration. *Biomed. Res. Int.* **2014**, 239356 (2014).
36. Jindarojanakul, P. et al. Changes in superoxide dismutase 3 (SOD3) expression in periodontal tissue during orthodontic tooth movement of rat molars and the effect of SOD3 on in vitro hypoxia-exposed rat periodontal ligament cells. *Eur. J. Orthod* **45**, 430–437 (2023).
37. Ongprakobkul, N. et al. Effects of local vs systemic administration of CXCR4 inhibitor AMD3100 on orthodontic tooth movement in rats. *Am. J. Orthod. Dentofac. Orthop.* **162**, 182–192 (2022).
38. Abuohashish, H. et al. Bevacizumab, a vascular endothelial growth factor inhibitor, promotes orthodontic tooth movement in an experimental rat model. *Heliyon* **9**, e16217 (2023).
39. Ma, D. et al. Asperosaponin VI injection enhances orthodontic tooth movement in rats. *Med. Sci. Monit.* **26**, e922372 (2020).
40. Suzuki, S. S. et al. Low-level laser therapy stimulates bone metabolism and inhibits root resorption during tooth movement in a rodent model. *J. Biophotonics* **9**, 1222–1235 (2016).
41. Xu, X., Zhou, J., Yang, F., Wei, S. & Dai, H. Using micro-computed tomography to evaluate the dynamics of orthodontically induced root resorption repair in a rat model. *PLoS ONE* **11**, e0150135 (2016).
42. Chen, S. et al. Contribution of diabetes mellitus to periodontal inflammation during orthodontic tooth movement. *Oral Dis.* **30**, 650–659 (2022).

Acknowledgements

The authors thank Dr. Makito Sakurai at the Institute of Science Tokyo, for technical assistance with the experiments involving the hypoxic animal chamber.

Author contributions

K.P.: conceptualisation, data curation, formal analysis, investigation, visualisation, validation, and writing (draft). Y.K.: conceptualisation, data curation, funding acquisition, investigation, methodology, project administration, supervision, validation, visualisation, and writing (draft, review, and editing). L.Y.: data curation, formal analysis, investigation, methodology, and writing (review and editing). Y.N.: conceptualisation, funding acquisition, methodology, and writing (review and editing). J.C.: project administration, supervision, and writing (review and editing). K.M.: conceptualisation, funding acquisition, project administration, resources, supervision, and writing (review and editing). All authors have reviewed and approved the final manuscript.

Funding

This work was supported by a JSPS KAKENHI Grant-in-Aid for Scientific Research (JP 23K27800 to K.M.) and a scholarship from the 100th Anniversary Chulalongkorn University Fund for Doctoral Scholarship.

Declarations

Competing interests

The authors declare no competing interests.

Additional information

Supplementary Information The online version contains supplementary material available at https://doi.org/10.1038/s41598-025-07949-9.

Correspondence and requests for materials should be addressed to Y.K.